Delivery of Peptide Coacervates to Form Stable Interaction Hubs In Cells

Wangjie Tu[1], Rachel Theisen[2], Amish Patel[3], Matthew C. Good[1,2,4*]

[1] Bioengineering Graduate Group, University of Pennsylvania, PA 19104
[2] Department of Cell and Developmental Biology, University of Pennsylvania, PA 19104
[3] Chemical and Biomolecular Engineering Department, University of Pennsylvania, PA 19104
[4] Department of Bioengineering, University of Pennsylvania, PA 19104

* Correspondence: mattgood@pennmedicine.upenn.edu

Abstract
Cells contain membrane-bound and membraneless organelles that operate as spatially distinct biochemical niches. However, these subcellular reaction centers lose fidelity with aging and as a result of disease. A grand challenge for biomedicine is restoring or augmenting cellular functionalities. Although commonly tackled by gene replacement therapy, an excited new strategy is the delivery of protein-based materials that can directly interact with and alternative biological networks inside a cell. In this study we sought to develop long-lasting materials capable of cellular uptake and incorporation, akin to an artificial organelle or intracellular interaction hub. Drawing inspiration from protein-based membranelles organelles we developed a new delivery method to transplant micron size peptide compartments into living cells. We determined conditions to form large stable coacervates that are efficiently taken up by a variety of useful cell types and demonstrate their intracellular stability over time. We developed tools to enhance the extent and spatial organization of cargo loading into these coacervates, including co-assembly of nanobodies that selectively bind to targets of interest. Combining them together, we demonstrate successful targeting of GFP-tagged cargo inside cells. These results represent an important first step toward the development of deliverable synthetic organelles that can be fabricated in vitro and taken up by cells for applications in cell engineering and regenerative medicine.

Keywords
Synthetic hubs, designer organelles, coacervate delivery, disordered peptide

Introduction

A grand challenge for biomedicine is achieving predictable control over cellular functions by controlling protein networks inside cells. In nature, cells utilize spatial partitioning via anchoring and scaffold proteins and leverage subcellular compartmentalization as key strategies to enhance the efficiency of biochemical processes. We have previously demonstrated the feasibility of controlling cellular processes and cell behavior by expressing proteins capable or forming synthetic membraneless organelles and targeting endogenous enzymes. However, to date this has required gene delivery using viruses or nanoparticles. A major advance would be the ability to fabricate compartments ex vivo and deliver them into cells to stably function as designer synthetic hubs or organelles.

Cells control the rate and fidelity of biochemical reactions by compartmentalizing components in membrane-bound and membraneless organelles. For example, oxidative phosphorylation is caried out in lipid bilayer containing mitochondria[1], and membraneless organelles such as the nucleolus specifically govern rRNA processing[2]. Stress granules sequester 48S to downregulate protein translation[3] or Nck-N-WASP-Arp2/3 condensates in T cells to recruit Sos1 and Arp2/3 to create a reaction hub[4]. Membraneless compartments form the self-assembly of proteins and RNAs intro micron-size condensates driven via multivalent interactions[5–7]. Similar ideology can be adopted to generate new designer condensates or compartments to programmably control reaction pathways in a cell[8,9]. Often the proteins that participate in this self-assembly and condensation contain large disordered or low-complexity polypeptide sequences[10,11]. We created synthetic condensates by expressing a disordered scaffold in cells and used them to reprogram cell behaviors. For example, we built compartments that functioned as insulators, turning signal flow on or off, for to regulate growth and division or to polarize cytoskeleton organization[12]. Separately, synthetic condensates can be used as bioreactors to enhance signaling between components or generate new signaling cascades among factors that normally only weakly interact[13]. However, there are a number of limitations of these studies for clinical applications. Gene delivery is required, gene expression has a maximum that limits the amount of condensed material (expression relative to c_{sat}), and native targets must be tagged to drive their localization to the synthetic condensate. We sought to overcome these hurdles using a novel strategy for protein-based delivery, using peptide coacervates.

There are a variety of strategies to achieve protein or nucleic acid delivery to cells. Commonly the RNA for a target of interest is delivered via lipid nanoparticles, which then drives expression inside a cells[14]. However it is not feasible to achieve very high protein expression with these methods[15], which limits their utility for delivering materials to form protein condensates that function as synthetic organelles. Cell permeable peptides exist in nature and have been designed that are capable of crossing the plasma membrane[16,17]. Although useful for drug delivery, these short peptide sequences cannot simply be appended to target proteins of interest to drive their cellular uptake. Recently, a promising new strategy for protein delivery has emerged based on identification of peptide coacervate particles capable of crossing the plasma membrane for cellular uptake[18]. The novel 26 amino acid disordered peptide HBpep was recently identified and shown capable of self-assembly into micron size coacervates through liquid-liquid phase separation[18–20]. These particles readily cross the cell membrane for cytosolic delivery. Its sequence consists of GHGVY GHGVY GHGPY GHGPY GHGLY W. These coacervates can be co-assembled or loaded with cargos including proteins and RNAs and will partially disassemble upon entering the cells, highlighting their utility for efficiency cytosolic delivery macromolecules[18,21]. Peptide variants such as HBpep-SA and HBpep-SP allow faster cargo release[18] and HBpep(GP)-SP and HBpep(RPY)-SP show different viscosity and cellular uptake kinetics[22]. Although primarily designed for drug delivery, we reasoned that the HBpep platform

could be adapted to create stable protein-based hubs or organelles in cells, creating a new toolbox to augment or revitalize cellular functions.

In this study, we created a new platform to form large coacervates capable or uptake and stable maintenance inside living cells. We developed strategies to enhance protein cargo loading and topological organization in coacervates, moving beyond passive loading and uniform partitioning. In contrast to previous controlled release systems, we developed strategies to deliver micro-size coacervates to cells that can serve as synthetic hubs or compartments, stable for days. Further we embedded nanobodies within these coacervated and demonstrated them capable of interfacing with protein targets in vitro and in cells. Delivery of synthetic hubs capable of targeting native enzymes and signaling pathways provides a powerful new strategy for applications in cellular engineering. By eliminating the requirement to deliver genetic material, this modular platform promises to fast-track therapeutic development, for example through formation of degradomes or via compartments that rewire aberrant signaling responses.

Results

Parameter optimization to form stable micron-size protein coacervates

Building from a previous peptide coacervated platform, HBpep[19,21], we sought to develop a protocol to form gel-like particles that range in size from 1-5 μm diameter for cargo loading and cellular uptake, and that could ultimately serve as stable synthetic 'hubs' or 'organelles' in a cell. We chose to promote nucleation and cross the phase boundary using two different methods: pH shift and temperature shift. HBpep contains histidines and is largely soluble in acidic buffer, such as pH 4.5, but will phase separate at physiological pH 7.4 under standard conditions[21]. Further, HBpep displays upper critical solution temperature behavior and LLPS can be induced by shifting the temperature from 50°C to room temperature, 23°C. We also chose to test both the standard HBpep, which has only limited cargo release capability and a redox sensitive form HBpep-SA, that will release cargo into the cytoplasm of a cell[18].

We first measured coacervation via pH shift for HBpep and HBpep-SA over a range of peptide concentrations from 0.1 to 2 mg/ml, corresponding to approximately 70 – 700 micromolar. We found coacervate size and number depended on peptide concentration (**Fig 1A-C**), as expected[23]. Although smaller particles have utility for drug delivery applications, we were interested in formation of larger hubs that would be stably maintained in cells. At concentrations of 0.5 mg/ml or higher, the average HBpep particle diameter was larger than 2 μm and could range from 1-6 μm (**Fig 1B**). Similar results were attained with HBpep SA, although the sizes were slightly smaller. Interestingly, a higher fraction of the HBpep-SA peptide partitioned to the coacervates as measured by spin-down (**Fig S1A-B**), although in both cases at majority of the scaffold peptide was condensed when assembled at a concentration of 0.5 mg/ml. We separately tested induction of LLPS via temperature shift and observed similar size and numbers of particles compared to induction via pH shift (**Fig S1C-E**). During protocol optimization, we found that the free peptides in solutions at pH 7.4 were actually quite sticky and would foul surfaces of test tubes or imaging chambers over time. Particle production via pH shift is somewhat more reliable at creating dose-dependent coacervation and indicates use of acidic buffers for storage and handling of HBpep and HBpep-SA prior to assembly.

For coacervates to be useful for non-genetic delivery of 'hubs' to cells, they need to show gel-like material properties, and not require free peptide present in continuous phase to maintain their assembly. In contrast, liquid-like condensates of disordered proteins formed inside cells from gene expression can have high turnover because the protein is continuously expressed and maintained

by a pool of material in the cytosol[24]. We thus tested the extent to which coacervates were in a gel or more liquid-like state by measuring diffusion following fluorescence recovery after photobleaching (FRAP). Particles were co-assembled with tracer amounts of a FITC-labeled HBpep (FITC-HBpep) (**Figure S1F**) peptides and bleached using a 405 nm laser. Fluorescence recovery was very limited over time, for both types of peptides, indicating very slow diffusion and suggesting that these particles are gels (**Figure 1D,E**), as expected[22]. Recovery was slow both from full photobleaching of particles to measure recovery via diffusion from continuous phase, and when photobleaching a portion of the particle to measure diffusion inside the coacervate. We conclude it is feasible to generate particles of 1-5 μm in diameter using either method for to induce LLPS and that peptide concentration can be varied to tune average coacervate size. Given their gel-phase properties we expected it would be feasible to dilute them into new solutions without providing additional material in continuous phase and that they should be stable.

Enhanced cargo loading into peptide coacervates via selective partitioning

We wondered whether it would be feasibility to enhance selectivity and overall amount of cargo loaded into coacervates by tagging the cargo. Previous studies demonstrated non-specific entrapment or loading of cargos such as protein and RNA during assembly HBpep and HBpep-SA coacervates[25]. However, loading efficiency varies for different cargos and depends on HBpep peptide concentration[25]. Here, we explored increasing the specificity of cargo loading without having to adapt the cargo or change HBpep peptide concentration. We used GFP as a model folded protein cargo for this proof-of-concept test. To promote selective loading, we added a 25-amino-acid motif from HBpep (lacking tryptophan) to the C-terminus of GFP (GFP-HBP) (**Figure 2A**), generating the protein via recombinant expression and purification. We co-assembled the cargo via LLPS of HBpep and measured extent of loading. We compared loading of GFP vs GFP-HBP both for HBpep and HBpep-SA particles, in which particles were formed by pH shift. We found that HBpep enhanced cargo loading into coacervates (**Figure 2B-D**), without changing coacervate sizes. We observed a nearly 2- to 3-fold increase in internal concentration of cargo as measured by fluorescence microscopy (**Figure 2C, D**) and total partitioning as measured via sedimentation (**Figure S2A, B**). We conclude it is feasible to enhance the overall magnitude of loading and internal concentration of cargo by fusion of a HBP tag to a protein of interest. Under conditions in which cargos would compete, the tagging would provide additional selectivity.

We next wondered whether it would be feasible to control the topology of cargo loading, dictating its spatial partitioning in the coacervate. Cargo loading appears spatially uniform for coacervates formed via pH shift method, and in general cargos reach a higher internal amount in particles comparing LLPS of HBpep via pH versus temperature for HBpep (**Figure 1B**). Tagging greatly increases the partitioning of GFP to particles formed via temperature shift (**Figure 1C**). Interestingly, the HBP tag also dictates the topology of cargo partitioning. GFP shows spatially uniform partitioning within particles whereas GFP-HBP enriches at the particle surface (**Figure 1B, C**). We conclude it is possible to specify a core-shell organization of scaffold and cargo that would enable spatially partitioning discrete cargos and would be broadly useful for a variety of applications in drug delivery and cell engineering. Note, for the remainder of this study we utilize pH shift to generate particles with uniform loading.

Delivering micron size or larger coacervates to cells and characterizing their stability

A previous study focused on delivery of particles smaller than 1 μm to cells and for the purpose of cytosolic particle dissociation and cargo release[25]. However, in this study, we were interested in using the HBpep and HBpep-SA platforms as stable synthetic hubs or organelles inside cells. As a result, we wanted to test the feasibility of delivering larger condensates to cells and their stability following uptake inside cells.

We sought to identify conditions to for highly efficient uptake of large particles in a variety of cell types. This included a transformed human cell line for osteosarcoma, U2OS, a mouse melanoma cell line, B16-F10, and primary human innate immune cells, monocytes (**Figure 3A**). We pre-assembled particles at 0.5 mg/ml and diluted them in cell media from 1:10 to 1:3 and measured particle uptake after 4 hrs and 24 hrs. Cells were washed extensively after particle addition to remove those not delivered to cells. We observed generally highly efficient uptake by cells for both particles of HBpep and HBpep-SA, in a variety of cell types (**Figure 3A**). These particles were present in the cytosol, but not the nucleus (**Figure 3A**) and showed diffusive motion (***Supp Movie1***). At 1 day, we measured effective and robust uptake of particles formed at both 0.2 and 2 mg/ml, averaging nearly 40 particles per cell at higher concentrations (**Figure 3B-E**). Particle formulations include a range of sizes although those formed at 0.2 mg/ml, the mode for the distribution of diameters was less than 1 μm and those formed at 2 mg/ml were generally larger than 1 μm. Importantly there was a long tail of particle sizes at higher concentrations (2 mg/ml formulation), and cells given these formulations contained nearly 10-fold higher numbers of larger particles (> 2 μm diameter) (**Figure 3D, E**). In exemplary cases we found it possible to fill up the cytoplasm of a cell with ~100 particles (**Figure S3E, *Supp Movie 2***), a feat not possible from genetic expression of a coacervating protein. Therefore, it is feasible for larger coacervates to be efficiently taken up by cells.

In an effort to build stable hubs than can be delivered to cells, we were interested in the stability of the particles inside cells over time. Previous efforts focus on use of particles < 1 μm diameter for drug delivery that would partially disassemble in the cytoplasm[25]. We sought to test the stability of the intracellular coacervates, comparing formulations better suited for drug delivery versus those ideal for making stable hubs. Particles were generally more stable by day 5 for coacervates assembled at 2 mg/ml vs. 0.2 mg/ml, likely related to their larger sizes (**Figure 3B, D**). Indeed, if we just quantified larger particles (> 2 μm diameter), the number per cell was relatively constant over time (**Figure 3E**). In contrast smaller particles (< 2 μm diameter) were lost from cells for the 0.2 mg/ml formulation. A recent study suggests these coacervates cross the cell membrane via micropinocytosis which enables the uptake of large portions of extracellular material. We conclude that cells can readily take up large coacervates, do so efficiently and that these particles are stable intracellularly for at least 5 days. These results provide a roadmap toward delivery and maintenance of synthetic 'hubs' within living cells without the need for gene transfer.

Selective targeting of proteins to pre-formed coacervates using nanobodies in vitro

To be useful as a designer organelle or hub, coacervates must be functionalized with molecules that enable them to interface with native protein interaction networks or signaling pathways. Native membraneless organelles can function as insulators[12] – sequestering components – or as bioreactor compartments that co-localize components at elevated concentrations[4]. We previously demonstrated that synthetic condensates could be formed via expression of a scaffold protein in cells, and that they could function as insulators, targeting and partitioning native enzymes that were tagged with a complementary coiled coil[12]. In this study we wanted to go further: to deliver synthetic hubs extracellularly rather than via gene transfer and expression, and to embed nanobodies within them that could bind to a target of interest without needing to tag the target. It would then be possible to create a designer biochemical niche inside a cell through the delivery of a one-pot peptide coacervate platform.

To start, we tested the feasibility of targeting proteins to the peptide coacervates in vitro comparing those fashioned with or lacking a nanobody (**Figure 4A**). As a proof-of-concept we tested co-assembly and embedding of the nanobody VHH4 which binds with nanomolar affinity to GFP[26]. This nanobody is highly useful because many stable cell lines have been created that contain a GFP-fusion to a target protein of interest. To track nanobody loading using fluorescence

microscopy we fused it to mCherry (VHH4-mCherry), or also to the HBP targeting sequence (VHH4-mCherry-HBP). To form particles, these purified proteins were added a 1:10 mass ratio into formulations of 0.5mg/ml HBpep and HBpepSA. Both nanobody cargos enriched within the HBpep and HBpep-SA particles (**Figure 4B and S4A, C**). We also observed somewhat elevated loading of VHH4-mCherry-HBP into HBpep particles (**Figure S4A, C**), consistent with the results described in Figure 2.

Once particles were formed, we tested partitioning of GFP target protein added to pre-formed coacervates in an imaging microwell. Particles lacking a VHH4 nanobody did not enrich GFP and instead partially excluded it (**Figure 4B, C**); note partition coefficient of less than 1. Thus, cargo uptake is almost non-existent following coacervate formation. In contrast particles contain VHH4 nanobody enriched the GFP target at their interface (**Figure 4B**) and this enrichment or partition coefficient at the surface was approximately 2-to 4- fold (**Fig 4C, S4D**) dependent on the type of peptide and whether HBP was present or not on the nanobody. Note that the nanobody loading is relatively uniform throughout particles, and thus the surface targeting is not caused by spatial partitioning of nanobody to periphery. It was recently shown that these gel-like particles of HBpep and HBpep-SA have limited permeability for macromolecules larger than 2-10 kDA[27]. At 27 kDa in molecular weight, the target GFP would be expected to have limited diffusion inside the coacervate, during the course of our 30 min experiments, consistent with the ring-like GFP partitioning to our VHH4 containing coacervates (**Figure 4B, S4B**)

Although mostly surface recruitment was achieved for this in vitro test using VHH4 and GFP, it should be possible to achieve higher internal partitioning of molecules with smaller molecular weights or by allowing cargos to incubate with coacervates for longer periods of time. Notably for drug delivery, the cargo is already co-assembled with the particle as we show in Figure 2. To conclude, in this initial test we sought and found proof of feasibility for selective binding of target proteins to coacervates using nanobodies. We wanted to test these particles for targeting in living cells.

Target enrichment at synthetic protein hubs inside cells

It has been suggested that HBpep particles are taken up by cells through actin-mediated macropinocytosis and phagocytosis[20]. In such a process, the coacervates will be encapsulated by lipid membrane, which poses a potential challenge for binding of target protein proteins. Based on published and our own GFP delivery experiments using HBpep-SA particles (Fig S3D), some GFP can be released into the cytosol, which implies that there may be some stochastic escape from membrane encapsulation. However to further promote endosomal escape, we included TAT-HA2 assist peptide[28] in co-assembly of HBpepSA particles loaded with VHH4 nanobody or a control protein. As a test case, we used a U2OS cell line that was virally transduced to stably expressed GFP as a target protein.

To determine whether coacervates could function as hubs in cells we wanted to compare target GFP binding to control mCherry containing HBpep-SA particles versus those containing the VHH4-mCherry nanobody. In cells loaded with control particles, we observed that most coacervates excluded the target GFP (**Figure 5A, C**), showing a partition coefficient less than 1. In contrast for VHH4-mCherry group, although many coacervates did not sequester the target (likely due to presence of membrane), we saw a large significant jump in target binding (**Figure 5B, D**). In cells, enrichment indices between below 2 are often non-specific. For control mCherry particles target GFP enrichment was below this value in nearly every case; observed < 1% of time (**Figure 5E**). In contrast hubs containing VHH4-mCherry and TAT-HA2 assist peptide showed target GFP partitioning as high as high as 10-15-fold above cytosolic levels (**Figure 5D, S5A**). The percentage of condensates with GFP enrichment over 2 was approximately 11.5% for

particles co-assembled with VHH4-mCherry and TAT-HA2, representing an order of magnitude increase in target enrichment compared to control particles.

A surprising result from the in vivo test is the topology of GFP recruitment. In our previous in vitro experiment, VHH4-mCherry loaded condensates were only able to recruit GFP to the surface, limited by the small condensate pore size[27]. However, after HBpepSA condensates are taken up by cells, we observe target GFP recruitment to the hub interior (Fig 5B, D). This difference of recruitment topology between in vitro and in vivo experiment may imply that HBpepSA condensates are partially disassembled in cytosol, which increases the pore sizes and allow larger molecules such as GFP to diffuse in, though more testing is needed.

We conclude it is feasible to deliver nanobody coacervates to cells that can function for days as stable hubs, capable of targeting endogenously expressed proteins to the microcompartment. Limitations of the current study include only partial endosomal release, which requires further optimization. These results demonstrate a path toward remodeling protein interaction networks in living cells using synthetic hubs or organelles and represent a unique opportunity for cell engineering without the requirement for gene delivery.

Acknowledgements
We thank D. Chenoweth lab for supporting initial peptide synthesis, and A. Stout and the Penn CDB Microscopy Core for imaging support. This study was partially supported by the National Institute of Biomedical Imaging and Bioengineering grant, EB028320 (M.C.G.), by National Science Foundation (NSF) MRSEC Seed grant, DMR1720530 (M.C.G.) and a seed award from the Center for Precision Engineering for Health (CPE4H) at the University of Pennsylvania (M.C.G.)

Competing Interests.
The authors declare no competing interests.

Materials and Methods: see supplementary materials

Figure Legends

Figure 1: Assembly and size control of HBpep and HBpepSA gel-like peptide coacervates

(A) Images showing assembly of coacervate particles from HBpep and HBpepSA using pH shift method at different concentrations of peptide. Solutions were at room temperature, 100 mM NaCl and at pH 7.4. Scale bar: 10 µm. **(B)** Quantification of HBpep and HBpepSA coacervate diameters at different concentrations via pH shift method. **(C)** Quantification of average number of HBpep and HBpepSA coacervates upon assembly at different concentrations (number per 4616.2 μm^2 imaging area). **(D)** Fluorescence images over time of FITC labeled (1:100) HBpep and HBpepSA coacervates formed at 0.5 mg/ml via pH shift, following laser photobleaching. Scale bar: 5 µm. **(E)** Quantification of normalized fluorescence after FRAP, showing intensity within bleached region of FITC labeled HBpep and HBpepSA coacervates formed via pH shift. Green line: HBpep whole condensate FRAP. Green dash line: HBpepSA whole condensate FRAP. Blue line: HBpepSA partial condensate FRAP.

Figure 2: Enhanced cargo loading and topological partitioning using disordered peptide tags

(A) Scheme showing strategy to enhance selectivity of cargo loading: comparing of GFP vs tagged GFP-HBP loaded in HBpep condensates through pH shift (left) or temperature shift (right) method. **(B)** Images of cargo loading into coacervates: 0.1 mg/ml GFP or GFP-HBP co-assembled (loaded) into 0.5mg/ml HBpep or HBpepSA particles through pH or temperature shift. Scale bar: 10 µm. **(C)** Quantitation of cargo loading via normalized line scan, averaging GFP or GFPHBP in coacervates of similar size. n=5 from (B). **(D)** Quantification of fluorescence intensity of cargo loading for GFP and GFPHBP in HBpep or HBpepSA coacervates. Enrichment index: fluorescence intensity in coacervate divided by the continuous phase.

Figure 3: Stable delivery of peptide coacervates to mouse and human cells and clinically relevant cell types

(A) Fluorescence images of coacervate uptake in cell lines. 30ul of HBpep particles assembled at 1mg/ml or 30ul HBpepSA particles assembled at 0.5mg/ml were added to the cell media for human osteosarcoma line U2OS, B16-F10 murine melanoma cells, and primary human monocytes. Green: FITC labeled condensates. Red: Abcam Cytopainter Cell Membrane Staining. Blue: Nucleus, stained DNA (DAPI). Scale bar: 10 µm. **(B)(D)** Quantification of size and number of coacervate taken up per cells; for formulations of 20 µl 0.2 mg/ml or 10ul 2 mg/ml HBpepSA delivered to U2OS; following particles over the course of 5 days. Cell number, n=10. **(C)** Fluorescence images of U2OS cells with particles at day 1 and day 5. Scale bar: 10 µm. **(E)** Quantification of the number of large coacervates (diameter > 2 µm) per cell compared to smaller ones (diameter < 2 µm) for particles assembled at 2 mg/ml and 0.2 mg/ml HBpepSA. Cell number, n=10.

Figure 4: Selective binding of protein targets to nanobody containing coacervates in vitro

(A) Scheme to determine selectivity of target binding to mCherry loaded or VHH4-mCherry loaded HBpep coacervates. VHH4 nanobody binds GFP. **(B)** Fluorescence images of cargo (mCherry or VHH4 mCherry) and target protein (GFP) added following addition of 1uM target protein. scale

bar: 10 μm. **(C)** Quantification of the enrichment of target GFP to HBpepSA coacervates. enrichment index: intensity of fluorescence on particle surface division by surrounding solution.

Figure5: Delivered VHH4-HBpepSA 'Hubs' bind and enrich native target GFP protein

(A)(B) Representative fluorescence images of target binding to hubs inside U2OS cells stably expressing GFP, comparing mCherry control and VHH4(nanobody)mCherry-loaded coacervates. 30ul of coacervates formed from 0.5 mg/ml HBpepSA, coassembled with 0.1mg/ml mCherry or VHH4-mCherry were added to the cell media for U2OS cells and imaged at 24 hr. Cell boundaries are indicated by dashed gray line. Chosen 'hub' for line scan is indicated by white line. Scale bar: 10 μm. **(C)(D)** Line scans of coacervate hubs showing fluorescence enrichment in (A)(B). **(E)** Quantification: percentage of hubs that show target enrichment greater than 2.

Bibliography

1. McBride, H. M., Neuspiel, M. & Wasiak, S. Mitochondria: More Than Just a Powerhouse. *Curr. Biol.* **16**, R551–R560 (2006).
2. Boulon, S., Westman, B. J., Hutten, S., Boisvert, F.-M. & Lamond, A. I. The Nucleolus under Stress. *Mol. Cell* **40**, 216–227 (2010).
3. Buchan, J. R. & Parker, R. Eukaryotic Stress Granules: The Ins and Outs of Translation. *Mol. Cell* **36**, 932–941 (2009).
4. Su, Q., Mehta, S. & Zhang, J. Liquid-liquid phase separation: Orchestrating cell signaling through time and space. *Mol. Cell* **81**, 4137–4146 (2021).
5. Banani, S. F., Lee, H. O., Hyman, A. A. & Rosen, M. K. Biomolecular condensates: organizers of cellular biochemistry. *Nat. Rev. Mol. Cell Biol.* **18**, 285–298 (2017).
6. Guo, Q., Shi, X. & Wang, X. RNA and liquid-liquid phase separation. *Non-Coding RNA Res.* **6**, 92–99 (2021).
7. Langdon, E. M. & Gladfelter, A. S. A New Lens for RNA Localization: Liquid-Liquid Phase Separation. *Annu. Rev. Microbiol.* **72**, 255–271 (2018).
8. Programmable synthetic biomolecular condensates for cellular control | Nature Chemical Biology. https://www.nature.com/articles/s41589-022-01252-8.
9. Dai, Y., You, L. & Chilkoti, A. Engineering synthetic biomolecular condensates. *Nat. Rev. Bioeng.* **1**, 466–480 (2023).
10. Piovesan, D. *et al.* MobiDB: 10 years of intrinsically disordered proteins. *Nucleic Acids Res.* **51**, D438–D444 (2023).
11. Fonin, A. V. *et al.* Biological soft matter: intrinsically disordered proteins in liquid–liquid phase separation and biomolecular condensates. *Essays Biochem.* **66**, 831–847 (2022).
12. Garabedian, M. V. *et al.* Designer Membraneless Organelles Sequester Native Factors for Control of Cell Behavior. *Nat. Chem. Biol.* **17**, 998–1007 (2021).
13. Sang, D. *et al.* Condensed-phase signaling can expand kinase specificity and respond to macromolecular crowding. *Mol. Cell* **82**, 3693-3711.e10 (2022).
14. Recent advances in mRNA-LNP therapeutics: immunological and pharmacological aspects | Journal of Nanobiotechnology. https://link.springer.com/article/10.1186/s12951-022-01478-7.
15. Müller, J. A. *et al.* Kinetics of RNA-LNP delivery and protein expression. *Eur. J. Pharm. Biopharm.* **197**, 114222 (2024).
16. Lindgren, M. *et al.* Cell-penetrating peptides. *Trends Pharmacol. Sci.* **21**, 99–103 (2000).
17. Liu, M., Fang, X., Yang, Y. & Wang, C. Peptide-Enabled Targeted Delivery Systems for Therapeutic Applications. *Front. Bioeng. Biotechnol.* **9**, (2021).

18. Sun, Y. *et al.* Phase-separating peptides for direct cytosolic delivery and redox-activated release of macromolecular therapeutics. *Nat. Chem.* **14**, 274–283 (2022).
19. Lim, J. *et al.* Liquid–Liquid Phase Separation of Short Histidine- and Tyrosine-Rich Peptides: Sequence Specificity and Molecular Topology. *J. Phys. Chem. B* **125**, 6776–6790 (2021).
20. Shebanova, A. *et al.* Cellular Uptake of Phase-Separating Peptide Coacervates. *Adv. Sci.* **11**, 2402652 (2024).
21. Sun, Y. *et al.* Redox-Responsive Phase-Separating Peptide as a Universal Delivery Vehicle for CRISPR/Cas9 Genome Editing Machinery. *ACS Nano* **17**, 16597–16606 (2023).
22. Sun, Y. *et al.* Phase-separating peptide coacervates with programmable material properties for universal intracellular delivery of macromolecules. *Nat. Commun.* **15**, 10094 (2024).
23. Gudlur, S. *et al.* pH-dependent interactions of coacervate-forming histidine-rich peptide with model lipid membranes. *Front. Soft Matter* **3**, (2024).
24. Bentley, E. P., Frey, B. B. & Deniz, A. A. Physical Chemistry of Cellular Liquid-Phase Separation. *Chem. – Eur. J.* **25**, 5600–5610 (2019).
25. Sun, Y. *et al.* Phase-separating peptides for direct cytosolic delivery and redox-activated release of macromolecular therapeutics. *Nat. Chem.* **14**, 274–283 (2022).
26. Kubala, M. H., Kovtun, O., Alexandrov, K. & Collins, B. M. Structural and thermodynamic analysis of the GFP:GFP-nanobody complex. *Protein Sci. Publ. Protein Soc.* **19**, 2389–2401 (2010).
27. Lim, J. *et al.* Hierarchical structural organization in bioinspired peptide coacervate microdroplets. 2024.07.06.602323 Preprint at https://doi.org/10.1101/2024.07.06.602323 (2024).
28. Wadia, J. S., Stan, R. V. & Dowdy, S. F. Transducible TAT-HA fusogenic peptide enhances escape of TAT-fusion proteins after lipid raft macropinocytosis. *Nat. Med.* **10**, 310–315 (2004).

Figure 1

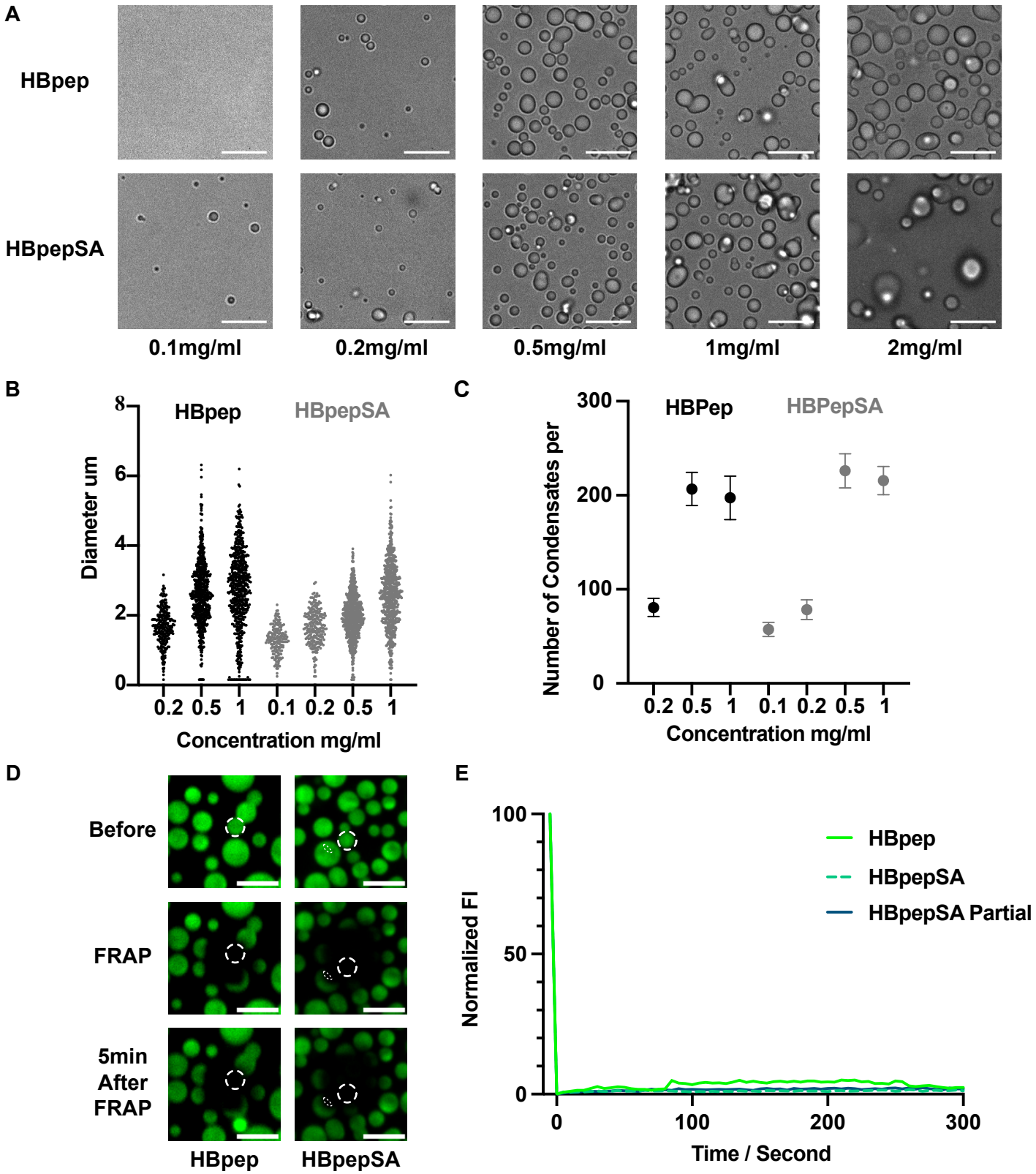
A
HBpep
HBpepSA
0.1mg/ml
0.2mg/ml
0.5mg/ml
1mg/ml
2mg/ml
B
HBpep
HBpepSA
Diameter um
0
2
4
6
8
0.2 0.5 1 0.1 0.2 0.5 1
Concentration mg/ml
C
HBPep
HBPepSA
Number of Condensates per
0
100
200
300
0.2 0.5 1 0.1 0.2 0.5 1
Concentration mg/ml
D
Before
FRAP
5min After FRAP
HBpep
HBpepSA
E
HBpep
HBpepSA
HBpepSA Partial
Normalized FI
0
50
100
0
100
200
300
Time / Second

Figure 2

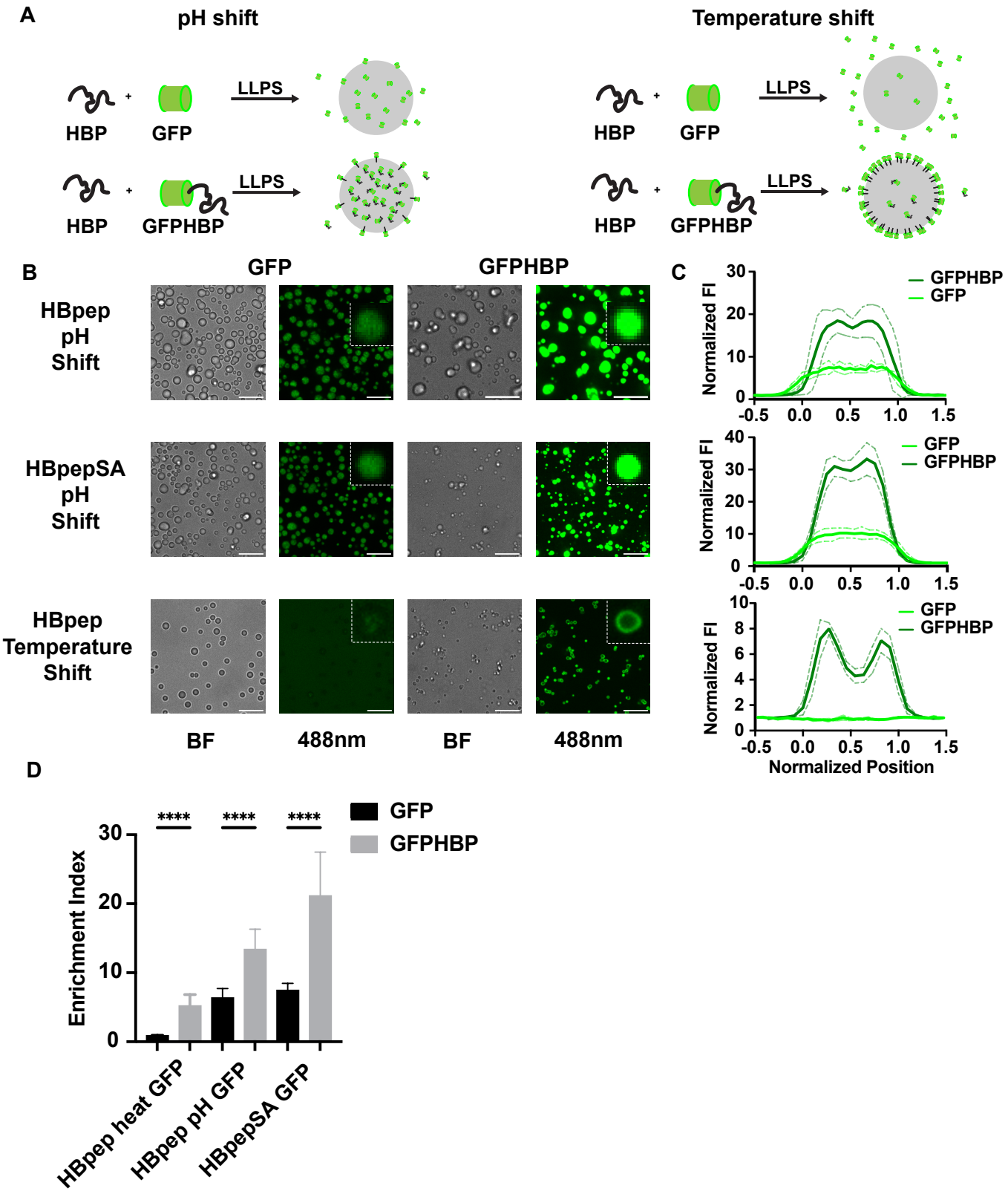
A
pH shift
Temperature shift
HBP
GFP
LLPS
HBP
GFPHBP
LLPS
HBP
GFP
LLPS
HBP
GFPHBP
LLPS
B
GFP
GFPHBP
HBpep pH Shift
HBpepSA pH Shift
HBpep Temperature Shift
BF
488nm
BF
488nm
C
GFPHBP
GFP
Normalized FI
Normalized Position
D
GFP
GFPHBP
Enrichment Index
****
****
****
HBpep heat GFP
HBpep pH GFP
HBpepSA GFP

Figure 3

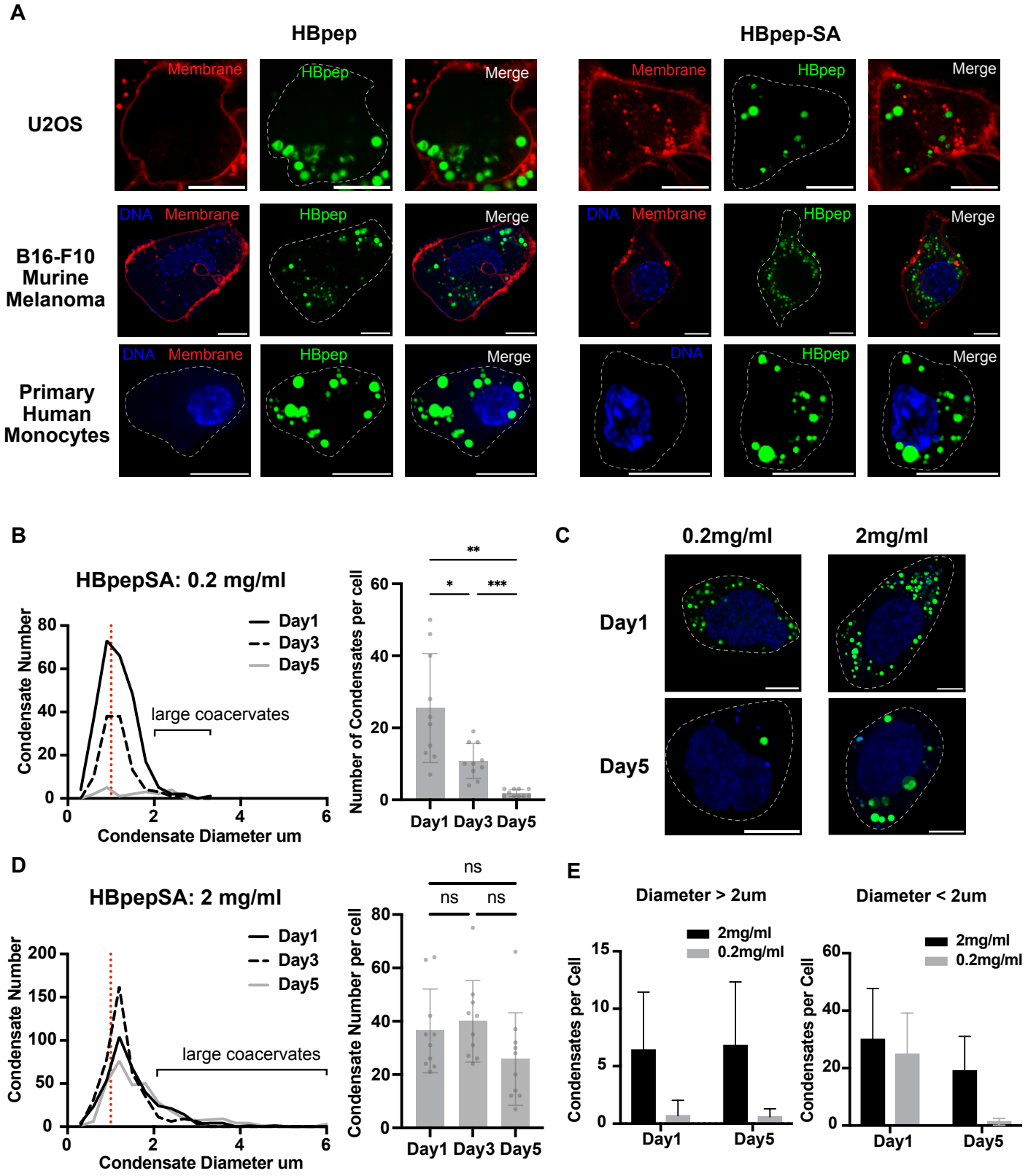
A
HBpep
HBpep-SA
U2OS
B16-F10 Murine Melanoma
Primary Human Monocytes
DNA
Membrane
HBpep
Merge
B
HBpepSA: 0.2 mg/ml
Condensate Number
Condensate Diameter um
Day1
Day3
Day5
large coacervates
Number of Condensates per cell
Day1 Day3 Day5
C
0.2mg/ml
2mg/ml
Day1
Day5
D
HBpepSA: 2 mg/ml
Condensate Number
Condensate Diameter um
Condensate Number per cell
ns
E
Diameter > 2um
Diameter < 2um
2mg/ml
0.2mg/ml
Condensates per Cell
Day1
Day5

Figure 4

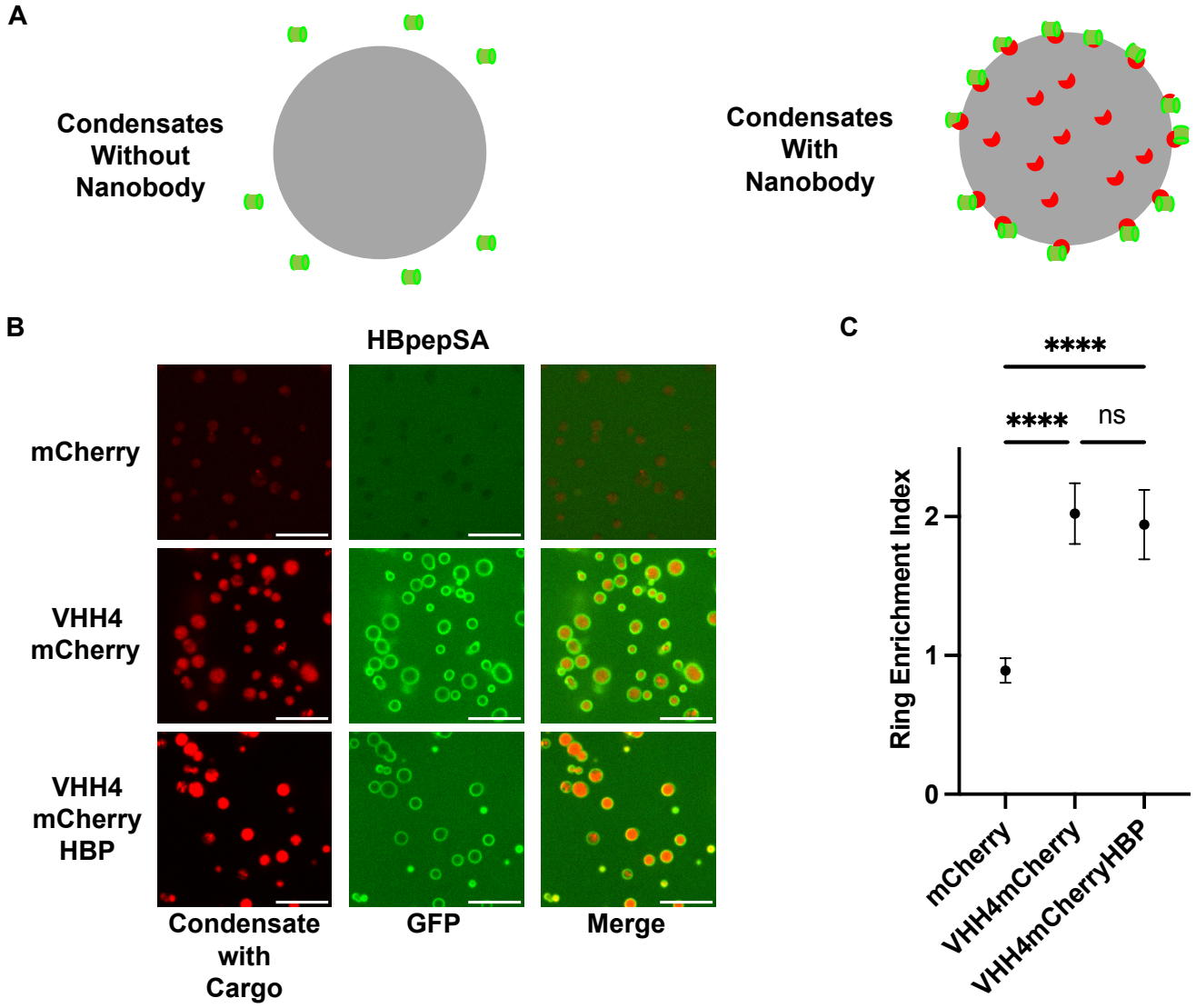
A
Condensates Without Nanobody
Condensates With Nanobody
B
HBpepSA
mCherry
VHH4 mCherry
VHH4 mCherry HBP
Condensate with Cargo
GFP
Merge
C
****
****
ns
Ring Enrichment Index
0
1
2
mCherry
VHH4mCherry
VHH4mCherryHBP

Figure 5

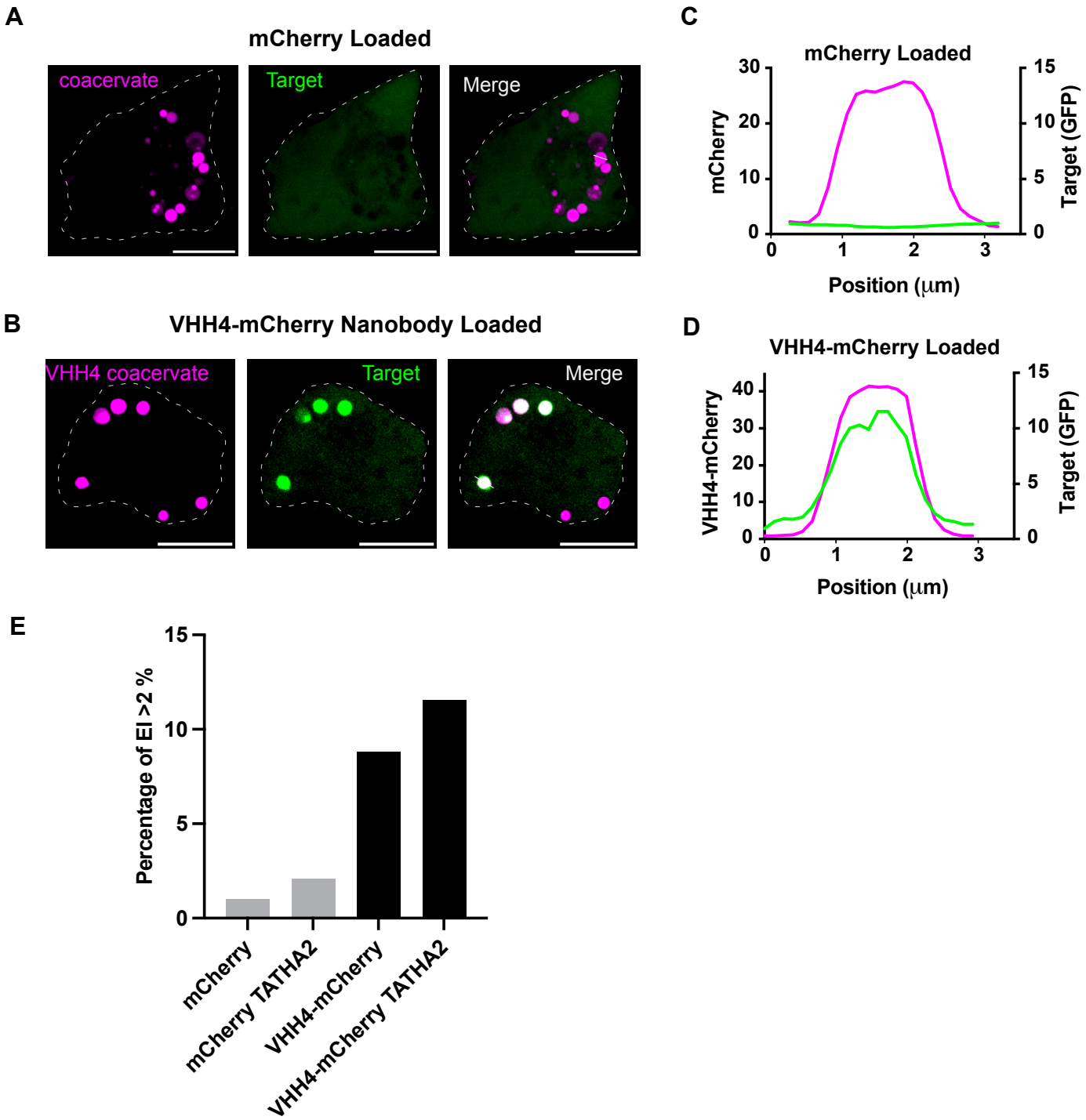
A
mCherry Loaded
coacervate
Target
Merge
B
VHH4-mCherry Nanobody Loaded
VHH4 coacervate
Target
Merge
C
mCherry Loaded
mCherry
Target (GFP)
Position (μm)
D
VHH4-mCherry Loaded
VHH4-mCherry
Target (GFP)
Position (μm)
E
Percentage of EI >2 %
mCherry
mCherry TATHA2
VHH4-mCherry
VHH4-mCherry TATHA2